Molecular Therapy
Nucleic Acids
Original Article

# Design, validation, and functional impact of oligonucleotides for multigene silencing in Alzheimer's disease

Caroline Woffindale,[1,2] Natalia Galindo Riera,[1,3] Matthew J.A. Wood,[1,2] and Miguel A. Varela[1,2,4]

[1]Department of Paediatrics, Institute of Developmental and Regenerative Medicine (IDRM), University of Oxford, Roosevelt Dr, Oxford OX3 7TY, UK; [2]MDUK Oxford Neuromuscular Centre, University of Oxford, Oxford, UK; [3]Molecular, Cellular and Genomic Biomedicine, Health Research Institute La Fe, 46026 Valencia, Spain; [4]Radcliffe Department of Medicine, University of Oxford, John Radcliffe Hospital, Level 6, West Wing, Oxford OX3 9DU, UK

**Alzheimer's disease (AD) is characterized by overlapping pathological processes, including amyloid-beta (Aβ) accumulation, tau hyperphosphorylation, mitochondrial dysfunction, and neuroinflammation. Monogenic therapies have shown limited benefits, and only in a subset of patients, as other pathological processes continue to drive disease progression. Given the multifactorial and heterogeneous nature of AD, therapeutics targeting more than one gene simultaneously represent a promising strategy to achieve broader therapeutic outcomes. This study highlights the advantages of multigene RNA-based therapeutics, which may overcome compensatory mechanisms and patient heterogeneity. Here, we report the design and functional validation of antisense oligonucleotides (ASOs) specifically engineered for simultaneous silencing of more than one AD-related gene. Using algorithm-assisted sequence design, we generated 11 bispecific gapmer ASOs from 20 candidate genes. In human and mouse cellular models, these ASOs achieved potent and sustained knockdown with picomolar to low-nanomolar $IC_{50}$ values. Functionally, treatment led to significant reductions in Aβ42 production, up to 70%, while maintaining favorable safety and specificity profiles. Collectively, our findings establish a proof of concept for multigene silencing in AD, demonstrating that rationally designed ASOs can provide robust target suppression across key pathological pathways. This strategy introduces a new paradigm in oligonucleotide design, with the potential to deliver disease-modifying benefits for patients with AD.**

## INTRODUCTION

Alzheimer's disease (AD) is the most common form of dementia, affecting millions worldwide and placing a significant burden on healthcare systems.[1] The hallmark neuropathological features of AD include the accumulation of extracellular amyloid-beta (Aβ) plaques and intracellular neurofibrillary tangles, leading to synaptic dysfunction and neuronal loss.[2,3] Despite decades of research, most current therapeutic strategies remain largely symptomatic and do not directly target the underlying molecular causes of the disease.[4,5]

Multiple therapeutic strategies have been widely researched to target genes implicated in AD pathogenesis, including the amyloid precursor protein (*APP*) and β-secretase (*BACE1*), which are critical for Aβ production.[6,7] However, lessons from recent anti-amyloid therapeutic trials suggest that silencing a single target may be insufficient to halt AD progression. Monotherapies focused solely on Aβ (for example, the anti-Aβ antibodies aducanumab and lecanemab) have shown limited efficacy, as patients often continue to deteriorate due to persistent tau pathology and other neurodegenerative processes.[8] This highlights the multifactorial nature of AD, wherein overlapping toxic cascades—such as amyloid deposition, tau hyperphosphorylation, mitochondrial dysfunction, and neuroinflammation—drive disease progression. In such a heterogeneous context, a combination approach that concurrently addresses multiple pathological pathways is increasingly viewed as necessary for durable therapeutic benefit.[9,10] By targeting parallel disease mechanisms, a multigene silencing strategy could produce synergistic effects and mitigate compensatory mechanisms that undermine single-target interventions.

RNA-based therapeutics have emerged as powerful modalities for precise and direct modulation of pathogenic gene expression. RNA interference (RNAi) technologies, including synthetic small interfering RNAs (siRNAs) and plasmid-based short hairpin RNAs (shRNAs), have enabled targeted silencing of individual genes of interest, and their therapeutic potential has been extensively explored in AD models. For example, RNAi-mediated silencing of *APP* and β-secretase (*BACE1*), key mediators of Aβ generation, has demonstrated promise in reducing pathogenic amyloid production.[7,11] Nevertheless, as with other therapeutic strategies, their long-term efficacy may be undermined by compensatory gene-regulatory mechanisms inherent to complex and multifactorial disorders such as AD.[12,13]

Received 26 September 2025; accepted 22 January 2026;
https://doi.org/10.1016/j.omtn.2026.102848.

**Correspondence:** Miguel A. Varela, Radcliffe Department of Medicine, University of Oxford, John Radcliffe Hospital, Level 6, West Wing, Oxford OX3 9DU, UK.
**E-mail:** miguel.varela@paediatrics.ox.ac.uk

Another clinically validated RNA-based therapeutic strategy involves antisense oligonucleotides (ASOs) that recruit the endogenous RNase H enzyme to mediate targeted RNA cleavage, resulting in robust and sustained gene silencing.[14,15] This class of ASOs, commonly referred to as gapmers, has shown clinical promise in neurodegenerative diseases. A notable example is Tofersen (Qalsody), an RNase H-dependent gapmer indicated for the treatment of SOD1-associated amyotrophic lateral sclerosis (ALS).[16] Nusinersen is another example of an ASO already in the clinic. It is approved for the treatment of spinal muscular atrophy (SMA) and works through a splice-switching mechanism to promote the production of full-length SMN2 transcripts.[17] Similarly, long-acting ASOs correcting tau isoform imbalance have shown that durable efficacy can be achieved in chronic neurodegenerative conditions, with splicing correction persisting for 2 years after a single administration in mice.[18] To explore the concept of using ASOs as a tool for multigene targeting, we designed and screened ASOs capable of concurrently suppressing more than one gene involved in AD pathology. Here, we report the development, validation, and comparative evaluation of these silencing strategies in cellular models of AD, demonstrating their feasibility and highlighting their potential as a novel, disease-modifying therapeutic approach.

## RESULTS

### Design and initial screening of bispecific ASOs

In this study, we designed ASOs to simultaneously silence more than one gene from a set of 20 genes with experimental evidence indicating their involvement in AD pathology (Table S1). An algorithm for identifying overlapping sequences shared by candidate genes and amenable to gene silencing[19] was used, yielding 11 bispecific ASOs. Initially, a screening was performed in human embryonic kidney 293 (HEK293) cells expressing *APP* with the Swedish mutation (HEK293 APPswe) at 20 nM. Gene silencing results in HEK293 APPswe cells identified four ASOs capable of silencing both target genes simultaneously 48 h after ASO treatment, as measured by qPCR (Figure 1). Notably, potent silencing was observed after treatment with APGS, targeting *APP* and *GSK3β* (Figure 1A); BAMT, targeting *BACE1* and *MTOR* (Figure 1C); BATA, targeting *BACE1* and *MAPT*, the gene encoding tau protein, (Figure 1G); and GRBCA, targeting *GRIN2B* and *CASP9* (Figure 1H). Because *GRIA2* and *NOX4* mRNAs were not detectable, the GRAGSB and GRANO ASOs could not be evaluated in HEK293 APPswe cells.

Subsequently, we screened the bispecific ASOs in SH-SY5Y neuroblastoma cells at 20 nM. *CASP9*, *GRIA2*, *GRIN2B*, and *NOX4* mRNAs were not detectable in SH-SY5Y cells. Therefore, the following ASOs could not be evaluated in this cell line: GRAGSB, GRANO, GRBCA, and GSBRGB. Of the seven bispecific ASOs targeting genes with sufficient expression for screening, six downregulated both genes, as shown by qPCR 48 h after transfection (Figure 2). These ASOs were APGS (Figure 2A), BAMT (Figure 2C), and BATA (Figure 2G), as in HEK293 APPswe cells (see above), but also BAPP1 (Figure 2D), BAPP2 (Figure 2E), and BAPP3 (Figure 2F), all three targeting *BACE1* and *APP*. In the case of BACD (Figure 2B), the ASO was able to downregulate *CDK5R1* but not *BACE1*.

BAPP2 and BAPP3 notably included chemically incorporated abasic sites, allowing increased flexibility in oligonucleotide design. The introduction of abasic sites enabled the design of longer ASOs despite sequence mismatches between *APP* and *BACE1*. Unlike mismatched bases, abasic sites completely abolish base-stacking interactions and remove any possibility of forming wobble or suboptimal base pairs,[20] offering added flexibility in design without necessarily increasing off-target risk. Therefore, starting from the original BAPP1 14-mer, we introduced abasic sites to enable inclusion of additional nucleotides common to both *BACE1* and *APP* upstream of the binding site. BAPP2 included 15 nucleotides plus an abasic site, whereas BAPP3 included 16 nucleotides plus two abasic sites. Nevertheless, we did not observe improvements over BAPP1 after the inclusion of abasic positions in the ASO and the elongation of the binding site. Thus, BAPP1, BAPP2, and BAPP3 were able to silence both *BACE1* and *APP* in SH-SY5Y cells (Figures 2D, 2E, and 2F), whereas they silenced only *BACE1* in HEK293 APPswe cells (Figures 1D, 1E, and 1F). Therefore, based on silencing potency and the critical importance and complementarity of the targeted genes in AD pathology, the two lead compounds from the screening were APGS (targeting *APP* and *GSK3β*) and BAMT (targeting *BACE1* and *MTOR*).

### $IC_{50}$, time course, and viability analysis

To further characterize our two lead compounds, APGS and BAMT, we proceeded with dose-response, time course, and cell viability analyses. Both ASOs demonstrated potent, concentration-dependent gene silencing with $IC_{50}$ values in the picomolar to low-nanomolar range for at least 48 h post-transfection, with no cytotoxicity at therapeutic concentrations (Figures 3 and 4). In HEK293 APPswe cells, BAMT displayed an $IC_{50}$ for *BACE1* of 6.90 nM (Figure 3A) and an $IC_{50}$ for *MTOR* of 10.18 nM (Figure 3B). Silencing persisted for at least 72 h after treatment at 20 nM (Figure 3C). Reduction in cell viability was detected only at the two highest doses, 80 and 100 nM (Figure 3D). APGS had an $IC_{50}$ silencing for *APP* of 2.86 nM (Figure 3E) and an $IC_{50}$ for *GSK3β* of 1.82 nM (Figure 3F). Silencing persisted for at least 72 h after treatment at 20 nM (Figure 3G). A reduction in cell viability was observed from 20 nM onwards (Figure 3H). In SH-SY5Y cells, BAMT displayed an $IC_{50}$ for *BACE1* of 15.81 nM (Figure 4A) and an $IC_{50}$ for *MTOR* of 2.74 nM (Figure 4B). Silencing persisted for more than 72 h after treatment (Figure 4C), with no reduction in cell viability at any dose tested (up to 100 nM, Figure 4D). For ASO APGS, the $IC_{50}$ for *APP* was 1.60 nM (Figure 4E) and the $IC_{50}$ for *GSK3β* was 1.28 nM (Figure 4F). Silencing persisted for 72 h after treatment (Figure 4G), and dose-dependent reduction in cell viability was significant at doses >40 nM (Figure 4H).

### Bispecific ASOs suppress Aβ42 production

To investigate whether ASOs attenuate Aβ production, we first optimized an Aβ42 ELISA to quantify secreted peptide levels in HEK293

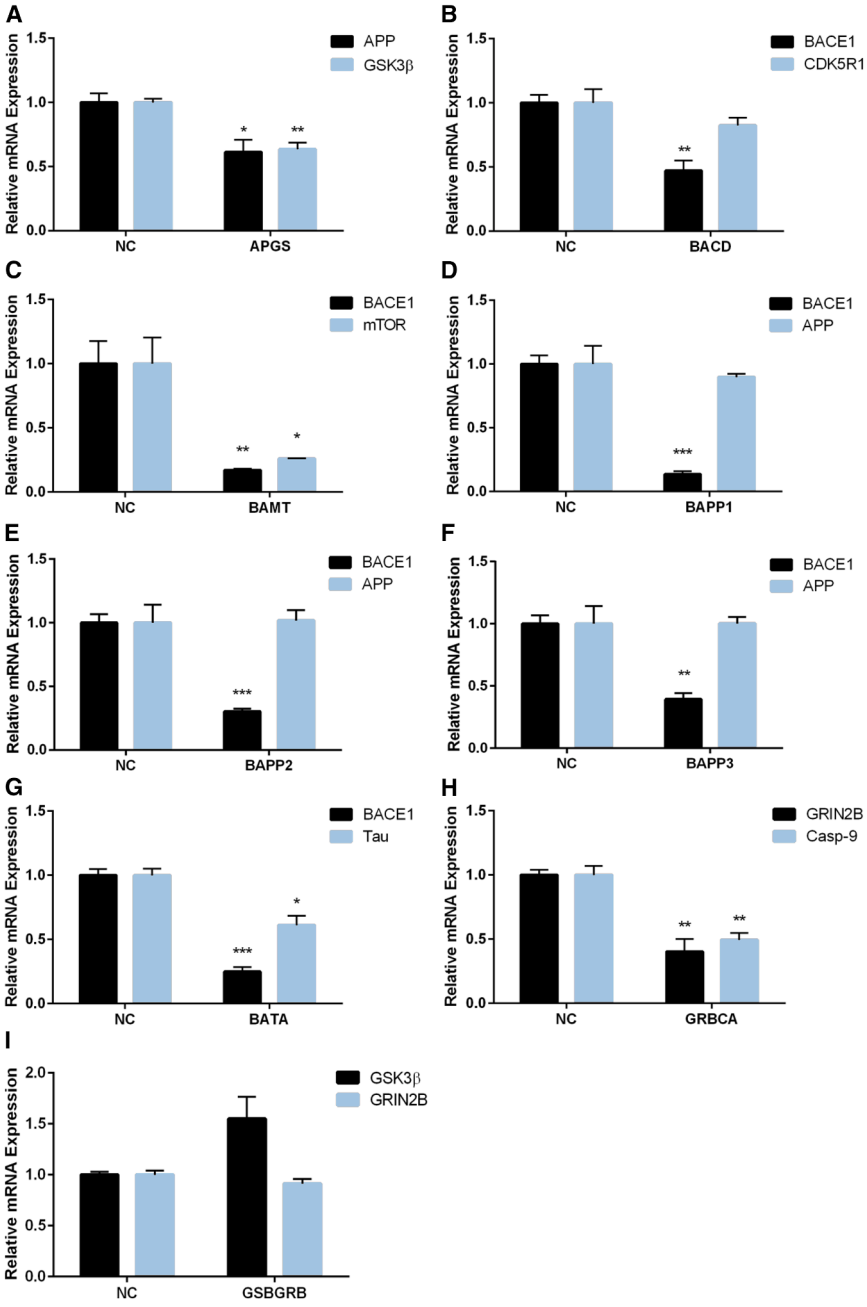


**Figure 1. Candidate bispecific ASO screening in HEK293 APPswe cells**

HEK293 APPswe cells were reverse-transfected with 20 nM of each candidate multigene ASO or a negative control ASO ("NC"). RNA was harvested after 48 h, and mRNA expression was assessed by qPCR, normalized to *ACTB* and *GAPDH*. Gene silencing observed following treatment with (A) APGS (*APP, GSK3β*), (B) BACD (*BACE1, CDK5R1*), (C) BAMT (*BACE1, MTOR*), (D) BAPP1 (*BACE1, APP*), (E) BAPP2 (BACE1, APP), (F) BAPP3 (BACE1, APP), (G) BATA (*BACE1, TAU*), (H) GRBCA (*GRIN2B, CASPASE-9*), and (I) GSBGRB (*GSK3β, GRIN2B*) multigene ASOs. Values are mean ± SEM, $n = 3$, $^{***}p < 0.001$, $^{**}p < 0.01$, $^{*}p < 0.05$, Student's *t* test.

APPswe and SH-SY5Y cells. After 48 h in culture, HEK293 APPswe cells secreted markedly higher amounts of Aβ42 than SH-SY5Y cells (Figure 5A). Analysis of cell lysates, concentrated supernatant, and supernatant diluted 1:5 confirmed that the secreted Aβ42 pool predominated and that unconcentrated samples required dilution to remain within the linear range of the assay. Having established these parameters, we assessed the effect of APGS and BAMT on Aβ42 production. HEK293 APPswe cells were reverse transfected with increasing concentrations of either APGS or BAMT, and supernatants were collected 48 h later for Aβ42 quantification. BAMT induced a potent, concentration-dependent inhibition of Aβ42, achieving a 75.6% reduction at 20 nM (Figure 5B), and markedly reduced expression of its intended targets, *BACE1* and *mTOR* (Figure 5C). Similarly, APGS treatment produced a robust, dose-dependent reduction in Aβ42, reaching an 89.3% decrease at 10 nM compared with negative control ASO (Figure 5D). This was accompanied by significant silencing of the target mRNAs, *APP* and *GSK3β* (Figure 5E). These results demonstrate that simultaneous silencing of key amyloidogenic pathways with ASOs effectively lowers extracellular Aβ42 levels in a human cellular model of AD. The concordance between Aβ42 suppression and target mRNA knockdown supports a mechanism driven by combined reduction of APP expression (APGS) or altered APP processing through BACE1 inhibition (BAMT).

### Aβ42 production is reduced to comparable levels by single-gene and bispecific targeting locked nucleic acid-ASOs

To assess the impact of targeting two separate genes simultaneously compared with silencing each alone, eleven single-gene ASOs were designed. These ASOs comprised similar chemistry to the bispecific ASOs but were predicted to individually target APP, GSK3β, BACE1, or mTOR (Table S2). HEK293 APPswe cells were reverse transfected with 10 nM of each single-gene ASO, the corresponding bispecific ASO, or a negative control ASO. The relevant mRNA expression, relative to β-actin, was assessed by qPCR after 48 h (Figure S2). This analysis showed successful single-gene targeting of mRNA expression at levels similar to those achieved by bispecific ASOs, specifically by APP-3 and GSK3β-2 (Figure S2A) and by BACE1-2, mTOR-1, and mTOR-3 (Figure S2B). APP-3, GSK3β-2, BACE1-2, and mTOR-3 were selected for further study.

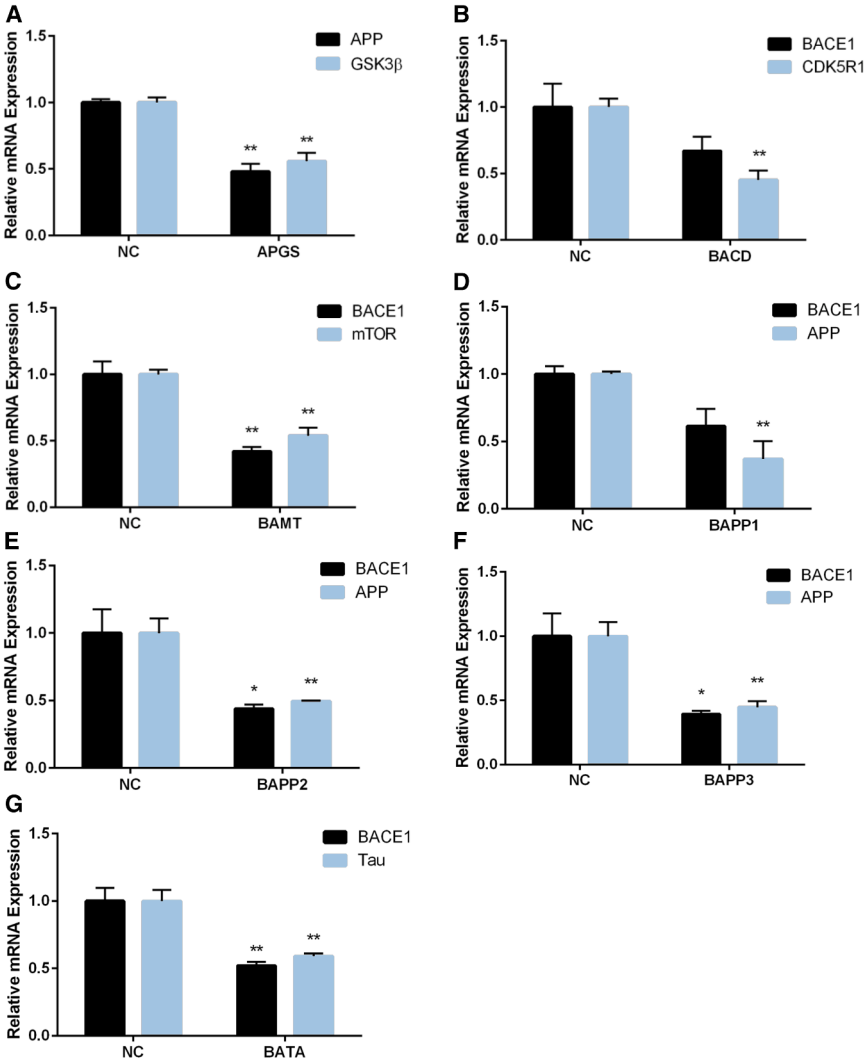


**Figure 2. Candidate bispecific ASO screening in SH-SY5Y cells**

SH-SY5Y cells were reverse-transfected with 20 nM of each candidate multigene ASO or a negative control ASO ("NC"). After 48 h, cells were harvested, and gene expression was assessed by qPCR, normalized to *ACTB* and *GAPDH*. Gene silencing observed following treatment with (A) APGS (*APP, GSK3β*), (B) BACD (*BACE1, CDK5R1*), (C) BAMT (*BACE1, MTOR*), (D) BAPP1 (*BACE1, APP*), (E) BAPP2 (BACE1, APP), (F) BAPP3 (BACE1, APP), and (G) BATA (*BACE1, TAU*) multigene ASOs. Values are mean ± SEM, $n = 3$, $^{**}p < 0.01$, Student's *t* test.

Subsequently, bispecific and single-gene ASOs targeting either APP and GSK3β (Figure S3) or BACE1 and mTOR (Figure S4) were compared for their ability to attenuate Aβ42 production. HEK293 APPswe cells were reverse transfected with either 10 nM of the APGS (Figure S3) or BAMT (Figure S4) multigene ASO, 10 nM of the corresponding single-gene ASOs, or a combination of either 5 or 10 nM of each corresponding single-gene ASO (i.e., 5/10 nM APP-3 and 5/10 nM GSK3β-2) to control for the multigene aspect. This analysis revealed that the APGS bispecific ASO resulted in a similar level of silencing of both mRNA and Aβ42 production as either APP-3 alone or the combination of 5/10 nM of APP-3 and GSK3β-2 single-gene ASOs (Figure S3). Correspondingly, the BAMT bispecific ASO also significantly silenced Aβ42 production to a similar extent as either BACE1-2 alone or the combination of 5/10 nM of BACE1-2 and mTOR-3 single-gene ASOs (Figure S4B), despite a slightly higher degree of silencing of BACE1 mRNA by BACE1-2 alone compared with the BAMT bispecific ASO (Figure S4A). Together, these results suggest that APGS and BAMT bispecific ASOs produce effective silencing of Aβ42 expression, with comparable efficacy to that elicited by single-gene ASOs.

Combination effects were initially interpreted under a Bliss independence framework. APP-3 single-gene targeting reduced relative Aβ42 levels to 0.2, while GSK3β-2 alone reduced Aβ42 to 0.7. Under Bliss independence, the expected additive effect of combined APP-3 and GSK3β-2 treatment would therefore be 0.14 remaining Aβ42 (calculated as $0.2 \times 0.7$). The observed Aβ42 level for the combined single-gene treatment was 0.3 at 5 nM each, indicating a less-than-Bliss effect, and 0.15 at 10 nM each, which closely approximated the Bliss-predicted value. Notably, the bispecific APGS ASO reduced Aβ42 to 0.25, a magnitude comparable to that achieved by combined single-gene targeting. Together, these observations suggest that bispecific ASO treatment is sufficient to recapitulate the additive effects of independent single-gene silencing within a single construct, without evidence of synergistic inhibition of Aβ42 production.

In addition, combination effects on Aβ42 were also assessed using a multiplicative additivity-based pharmacodynamic framework. For APP/GSK3β targeting, the observed reduction in Aβ42 following combined APP-3 and GSK3β-2 treatment at 10 + 10 nM was compared to the multiplicative additivity prediction derived from the corresponding single-agent effects, and the difference was tested using a two-sided difference-from-prediction z-test; no significant deviation from additivity was detected ($p = 0.9$). At equal total oligonucleotide mass (10 nM), the bispecific APGS was compared with the equal-mass monospecific mixture (5 + 5 nM) using a two-sided Welch's *t* test, revealing no significant difference in Aβ42 reduction ($p = 0.42$).

For BACE1/mTOR targeting, mTOR-3 alone did not reduce Aβ42, and multiplicative additivity therefore predicted a

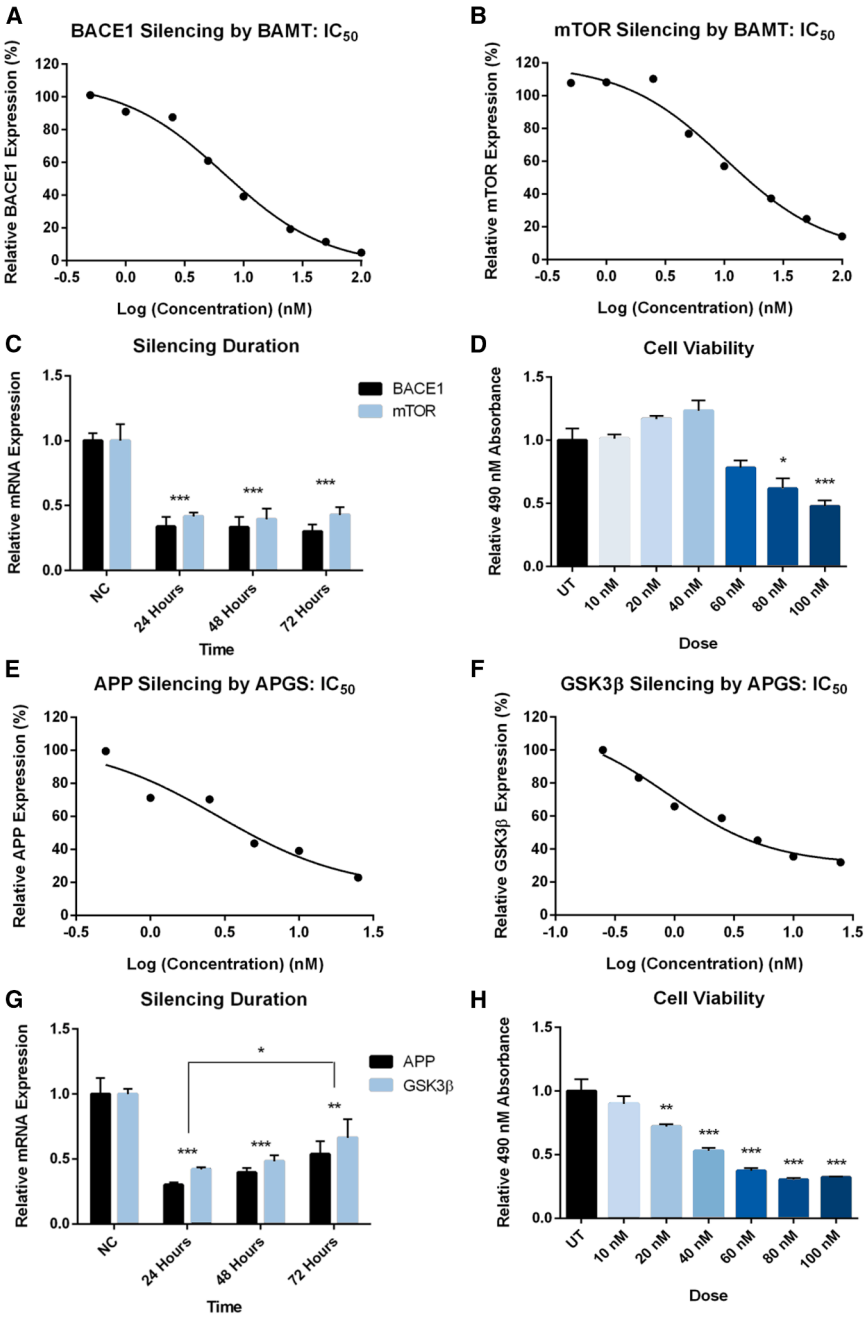


**Figure 3. Characterization of BAMT and APGS ASO silencing in HEK293 APPswe cells**

HEK293 APPswe cells were left untreated ("UT") or transfected with either BAMT (targeting *BACE1* and *MTOR*) or APGS (targeting *APP* and *GSK3β*) multigene ASOs, alongside corresponding negative control ASOs ("NC"). mRNA, normalized to *ACTB*, was assessed by qPCR 48 h post-transfection. Dose-response curves for *BACE1* and *MTOR* (BAMT) or *APP* and *GSK3β* (APGS) mRNA expression are shown relative to NC ASO treatments (10 nM). (A and B) $IC_{50}$ plots for BAMT-targeted genes: (A) *BACE1*, (B) *MTOR*. (E and F) APGS-targeted genes: (E) *APP*, (F) *GSK3β*. These plots illustrate ASO concentration-dependent silencing efficacy. A 4-parameter logistic (4PL) dose-response model was used to compute $IC_{50}$ values. The *x* axis shows the base-10 logarithm of ASO concentration in nanomolar (nM): Log = −1 (0.1 nM), Log = 0 (1 nM), Log = 1 (10 nM), Log = 1.5 (31.6 nM). (C, G) Time course analysis of gene silencing persistence was performed after transfection with 20 nM BAMT (C) or APGS (G), compared to NC controls. (D, H) Cell viability was determined by MTS assay 48 h post-transfection with each ASO. All values represent mean ± SEM, $n = 3$; statistical significance indicated by $^{***}p < 0.001$, $^{**}p < 0.01$, $^{*}p < 0.05$, determined by one-way ANOVA followed by Tukey's post-hoc test.

BACE1-dominated combination effect. The observed 10 + 10 nM mixture did not significantly deviate from this prediction when assessed by a difference-from-prediction z-test ($p = 0.40$). At equal total oligonucleotide mass (10 nM), comparison of the bispecific BAMT with the equal-mass monospecific mixture (5 + 5 nM) using a two-sided Welch's *t* test indicated a trend toward greater Aβ42 reduction with the monospecific mixture ($p = 0.055$). Collectively, these analyses support an additive model of action for combined targeting and indicate that bispecific constructs recapitulate Aβ42 lowering.

### Assessment of tau phosphorylation as a downstream readout of GSK3β and MTOR silencing

To investigate potential downstream pathway effects of GSK3β and MTOR silencing, we assessed tau phosphorylation at the Ser396 epitope (pS396), a site regulated by both kinases. Full experimental details and figures are provided in the Supplemental Material (Figures S5–S8).

In HEK293 APPswe cells, both APGS and BAMT produced a small reduction in tau pS396 as measured by ELISA; however, tau protein levels were extremely low, and pS396 was only weakly detectable by western blot (Figure S5A and S5B). These findings indicate that HEK293 APPswe cells are not optimal for tau-related readouts due to minimal baseline tau expression.

We therefore examined tau phosphorylation in SH-SY5Y cells, which express higher basal tau levels. In this model, APGS and BAMT again resulted in a modest reduction in tau pS396 protein levels after 48 h (Figures S6–S8). A slight decrease in

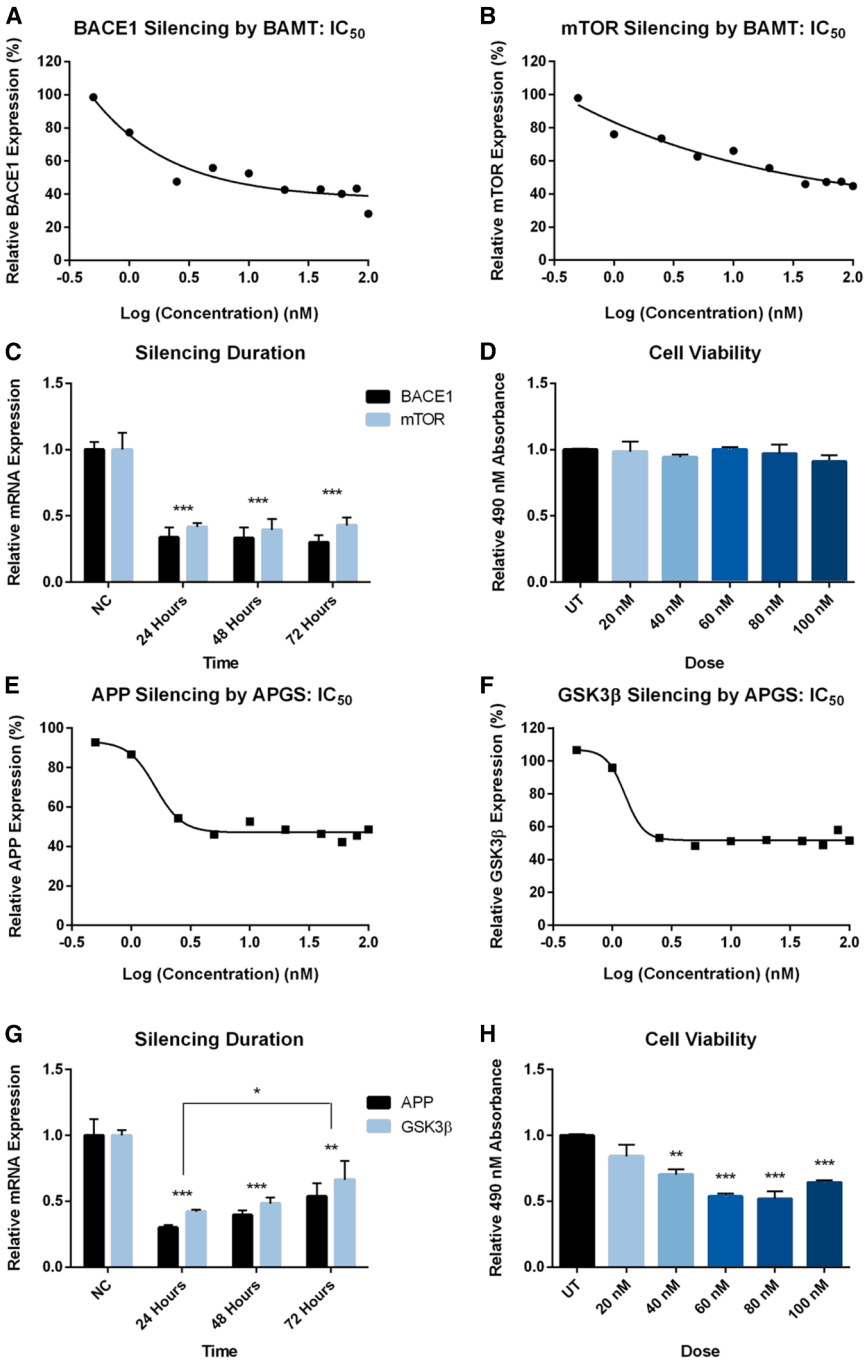


**Figure 4. Characterization of BAMT and APGS ASO silencing in SH-SY5Y cells**

SH-SY5Y cells were left untreated ("UT") or transfected with either BAMT, APGS, or a negative control ASO ("NC", 20 nM) at the indicated concentrations. mRNA, normalized to *ACTB*, was assessed by qPCR 48 h post-transfection. Dose-response curve of *BACE1* and *MTOR* mRNA expression following BAMT multigene treatment relative to NC ASO are shown. (A and B; E and F) $IC_{50}$ plots for (A) *BACE1* and (B) *MTOR* mRNA expression following BAMT multigene ASO treatment relative to NC, and (E) *APP*, (F) *GSK3β* mRNA expression following APGS treatment. We used a 4-parameter logistic (4PL) dose-response model to compute $IC_{50}$ values. Each value on the *x* axis corresponds to the base-10 logarithm of the drug concentration in nanomolar (nM) (Log = −1, 0.1 nM; Log = 0, 1 nM; Log = 1, 10 nM; Log = 2, 100 nM). (C, G) Duration of gene silencing following transfection of 20 nM BAMT (C), APGS (G), or NC ASOs after 24, 48, and 72 h (D, H) Cell viability assessed by MTS assay 48 h after BAMT (D) or APGS (H) ASO treatment. Values are mean ± SEM, $n = 3$, $^{***}p < 0.001$, $^{**}p < 0.01$, $^{*}p < 0.05$, one-way ANOVA followed by Tukey's post-hoc test.

total tau accompanied these effects, and tau mRNA levels showed a small but non-significant reduction across treatments, consistent with the limited magnitude of change observed by western blot.

These results suggest that while the dual-target ASOs may influence downstream pathways, immortalized cell lines present a restricted dynamic range for quantitative tau phosphorylation analyses. More physiologically relevant systems (e.g., induced pluripotent stem cell [iPSC]-derived neurons or *in vivo* models) will be required to determine the mechanistic consequences of multigene silencing on tau biology.

### Experimental assessment of target specificity

To minimize the risk of sequence similarity with other genes, candidate sequences were initially subjected to BLAST analysis. Target specificity was also experimentally assessed. *HN1* (hematological and neurological expressed 1) was selected as a potential off-target gene, as it contained a sequence differing from the target of our lead compound BAMT ASO by a single nucleotide (adenine instead of thymine at the penultimate position; CATTGTCTCTAAC). SH-SY5Y and HEK293 APPswe cells were reverse transfected with the BAMT ASO at varying concentrations (2.5, 10, and 25 nM), and *HN1* mRNA expression was quantified relative to *ACTB* at 48 h. No significant changes in *HN1* expression were observed in either cell line after treatment with BAMT (Figure S1).

### Validation of mBAMT in murine Neuro2A cells

Based on the positive outcomes of dose-response, time course, and cell viability analyses; the efficacy in reducing Aβ (Aβ42) levels; and the *in silico* and experimental characterization of possible

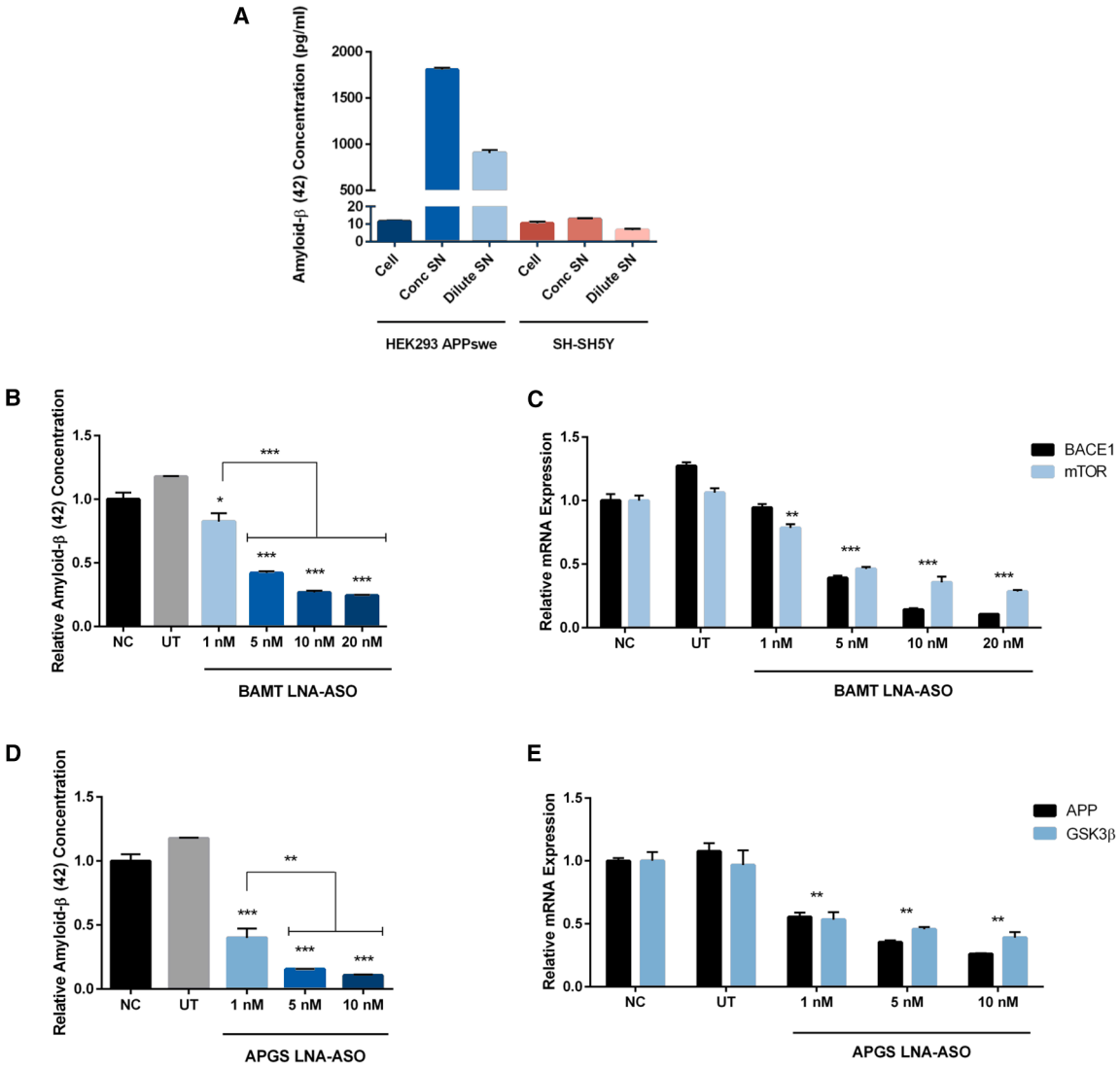


**Figure 5. Bispecific LNA-ASOs suppress amyloid-β(42) production in HEK293 APPswe cells**

(A) Quantification of basal amyloid-β(42) (Aβ[42]) secretion by HEK293 APPswe and SH-SY5Y cells by ELISA. Cell lysates are indicated as Cell, concentrated supernatant as Conc SN, and supernatant diluted 1:5 with kit diluent as Dilute SN. HEK293 APPswe cells secreted markedly higher Aβ42 than SH-SY5Y cells.

(B and C) Dose-dependent inhibition of Aβ42 production by BAMT multigene LNA-ASO. HEK293 APPswe cells were left untreated ("UT") or reverse transfected with a negative control ASO ("NC", 10 nM) or increasing doses of BAMT. Supernatant was collected after 48 h, diluted 1:1, and Aβ42 quantified by ELISA (B). *BACE1* and *MTOR* mRNA expression, normalized to *ACTB*, was measured by qPCR (C). (D and E) Dose-dependent inhibition of Aβ42 production by APGS multigene LNA-ASO. Cells were treated as in (B) and (C), and Aβ42 concentration was assessed by ELISA (D). *APP* and *GSK3β* mRNA expression, normalized to *ACTB*, was measured by qPCR (E). All values are mean ± SEM ($n$ = 3). Statistical significance was determined by one-way ANOVA followed by Tukey's post-hoc test: $^{*}p < 0.05$, $^{**}p < 0.01$, $^{***}p < 0.001$.

off-target effects, we chose BAMT as our lead compound. To further advance the preclinical development of this silencing strategy, we fully evaluated the efficacy of a mouse-specific version of our lead compound BAMT (mBAMT) in Neuro2A murine neuroblastoma cells at the mRNA and protein level. Treatment with mBAMT effectively reduced expression of mouse *Bace1* (Figure 6A) and *Mtor* (Figure 6B), demonstrating potent, concentration-dependent silencing with picomolar or low-nanomolar $IC_{50}$ values ($IC_{50}$ *Bace1* = 0.18 nM, $IC_{50}$ *Mtor* = 10.38 nM). Silencing persisted for 48 h after treatment (Figure 6C). Reduction in cell viability was only significant at the 100 nM dose (Figure 6D). Potent silencing of Bace1 and mTOR was also observed at the protein level (Figure 6E) 48 h after treatment, even at the lowest doses tested (1, 5, 10, 20, and 40 nM). These findings highlight the likely applicability

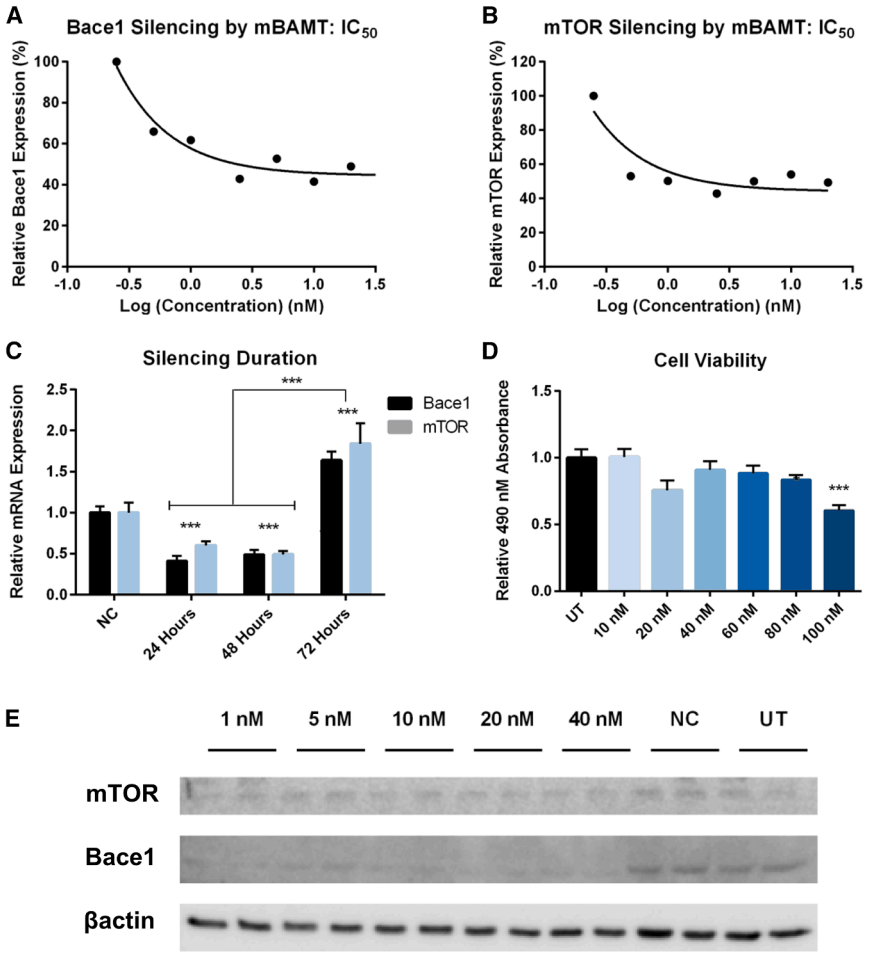


**Figure 6. Characterization of mBAMT multigene ASO in mouse Neuro2A cells**

Neuro2A cells were left untreated ("UT") or were reverse transfected with either the mBAMT multigene ASO or a negative control ASO ("NC") at the indicated concentrations. mRNA and protein expression, normalized to *Actb*, were assessed by qPCR after 48 h. $IC_{50}$ plots for (A) *Bace1* and (B) *Mtor* mRNA expression following mBAMT multigene ASO treatment relative to NC are shown. We used a 4-parameter logistic (4PL) dose-response model to compute $IC_{50}$ values. Each value on the *x* axis corresponds to the base-10 logarithm of the drug concentration in nanomolar (nM) (Log = −1, 0.1 nM; Log = 0, 1 nM; Log = 1, 10 nM; Log = 2, 100 nM). (C) Duration of gene silencing following transfection of 20 nM mBAMT or NC ASOs after 24, 48, and 72 h. (D) Cell viability assessed by MTS assay 48 h after mBAMT ASO treatment. (E) Western blot analysis of Bace1 and mTOR protein expression after mBAMT multigene ASO treatment, compared with NC and untransfected (UT) cells. Values are mean ± SEM, $n = 3$, $^{***}p < 0.001$, $^{**}p < 0.01$, $^{*}p < 0.05$, one-way ANOVA followed by Tukey's post-hoc test.

of this silencing strategy *in vivo* studies and showcase the potential to deliver disease-modifying benefits through this new paradigm in oligonucleotide design.

## DISCUSSION

Conventional monogenic therapeutic approaches have yielded limited clinical benefit in AD, frequently failing to account for the disease's inherent heterogeneity and compensatory biological responses. To address these limitations, this study explores a multigene targeting strategy utilizing rationally engineered bispecific ASOs. Through a systematic design framework informed by transcriptomic prioritization across 20 AD-associated genes, a panel of bispecific gapmer ASOs was developed and functionally validated. The resulting compounds achieved robust and sustained dual-gene silencing in both human and murine cellular models, with downstream reductions in Aβ42 levels. These findings position ASO therapy as a scalable and mechanistically grounded strategy to circumvent the limitations inherent to single-target interventions in AD.

This work provides proof-of-concept evidence that bispecific ASOs can achieve potent gene silencing (low nanomolar $IC_{50}$), capable of simultaneously suppressing more than one AD-relevant target to address the disease's inherent heterogeneity. A major advantage of this strategy is the ability to target contributors to AD pathology in parallel, potentially producing a combined therapeutic impact greater than that of individual, single-target treatments. By not being limited to a single pathway or cell type, this silencing strategy could broadly address the complex network of dysregulations characteristic of AD. For instance, the APGS ASO could simultaneously mitigate amyloidogenic processing through *APP* knockdown and reduce tau-related toxicity via *GSK3β* suppression.[21,22] Similarly, the BAMT ASO combines inhibition of *BACE1* (reducing Aβ production) with downregulation of *MTOR*, enhancing autophagic clearance of protein aggregates and modulating synaptic protein synthesis.[23–25] Such combined targeting, leading to attenuation of multiple toxic cascades, amyloid accumulation, kinase dysregulation, and impaired proteostasis, could extend therapeutic impact across different stages of disease progression.[26,27] This is particularly beneficial since certain pathologies, such as soluble Aβ oligomers, predominantly drive early synaptic dysfunction, whereas tau tangles and neuroinflammation typically dominate later stages.[28,29] Hence, bispecific ASOs might more effectively span these disease phases than therapies targeting a single pathway.

*MTOR* is a central regulator of autophagy, acting through downstream effectors such as p70 S6 kinase (p-S6K) to restrain autophagic flux under nutrient-replete conditions. Accordingly, a reduction in *MTOR* expression by the BAMT ASO would be expected to attenuate p-S6K activity and promote autophagy, potentially reflected by

increased LC3-II formation and reduced p62 accumulation, consistent with previous observations in tau-related models.[30] Although we did not quantitatively assess these autophagy markers in the present work, they represent an important mechanistic axis for future studies. More physiologically relevant systems, such as iPSC-derived neurons or *in vivo* AD models—where autophagy dysfunction and tau phosphorylation abnormalities are more pronounced—will be better suited to determine the extent to which simultaneous targeting of *BACE1+MTOR* or *APP+GSK3β* modulates these interconnected pathways.

A related advantage is the capacity of multigene approaches to counteract compensatory mechanisms. Biological networks commonly respond to inhibition of one node by adaptively upregulating parallel or alternative pathways.[19,31,32] By concurrently targeting parallel or downstream factors, such as *APP* or *MTOR*, a multigene ASO reduces the potential for biological networks to evade therapeutic intervention. Furthermore, AD patient heterogeneity necessitates broad-spectrum therapeutic approaches. AD pathology differs markedly across individuals; some patients exhibit a predominant tau burden relative to amyloid, while others present with significant vascular or inflammatory pathologies.[33–35] Therapeutics narrowly targeting only one aspect (e.g., amyloid deposition) may lack effectiveness in patients for whom other pathological mechanisms predominate. By contrast, multigene strategies can potentially provide broader therapeutic coverage, increasing the likelihood of clinical efficacy across diverse patient populations. This rationale has also motivated the development of receptor-level multi-target-directed ligands (MTDLs), such as those described by Turgutalp et al. (2022),[36] who demonstrated that rationally designed cholinesterase inhibitors with additional activity at σ1R, σ2R, NMDA receptors, and P2X7R achieved synaptoprotection and anti-inflammatory effects *in vivo*. These MTDLs, which outperformed donepezil, reinforce the therapeutic value of simultaneously engaging multiple pathogenic nodes, including through small molecules.

Additionally, brain cell-type heterogeneity contributes significantly to AD pathology, as neurons, microglia, and astrocytes each play distinct roles. For instance, while *BACE1* expression is largely neuronal, *GSK3β* and inflammatory pathways affect multiple cell types. ASOs targeting genes expressed across these cell types ensure broader engagement and may yield a more resilient, network-level therapeutic effect. This network-level impact could help maintain cognitive function even when certain pathological pathways are only partially modulated.

In essence, multigene ASOs aim to emulate endogenous regulatory systems, such as microRNAs (miRNAs), which fine-tune multiple gene targets simultaneously to maintain cellular homeostasis.[37,38] Recent integrative studies leveraging generative AI, bioinformatics, and single-cell transcriptomics highlight the genetic and immune complexity of AD, reinforcing the rationale for multi-target therapeutic strategies.[39] Like miRNAs, carefully designed multigene ASOs could restore balance within dysregulated networks by attenuating multiple pathogenic genes concurrently. Comparatively, chronic modulation of endogenous miRNAs carries inherent risks due to their broad transcriptome-wide targeting, potentially leading to unintended suppression of critical cellular pathways, including survival mechanisms or tumor suppressor signaling cascades.[40,41] Our engineered ASOs mitigate this risk by employing rigorous sequence design criteria to ensure specificity.

Our best-performing multigene ASO, BAMT, achieved approximately 70% reduction in Aβ production, demonstrating enhanced efficacy that could be attributable to simultaneous reduction in substrate availability and enzymatic activity within the amyloidogenic cascade.[11,42] This underscores the promise of ASO technology, which benefits from chemical modifications that confer stability and flexible multigene sequence design, as a durable therapeutic strategy for AD. Ongoing innovations in ASO chemistry, including stereopure PMO-gapmers with improved safety and stability for tau reduction, further exemplify how chemical design can enhance clinical translation.[43]

Nonetheless, a multigene approach presents certain challenges and limitations. Expanding target coverage must proceed cautiously to avoid unintended off-target gene suppression. Although we applied stringent criteria in our sequence design to minimize the risk of unintended binding, further comprehensive transcriptomic analyses *in vivo* are necessary to confirm specificity. Additionally, while we achieved effective dual-gene silencing, certain pathological aspects of AD, such as inflammation and oxidative stress, were not directly targeted. Incorporating additional therapeutic targets in future designs, or resorting to cocktails of molecules, may offer further benefits. Even if a cocktail strategy is pursued, our targeting designs minimize the number of therapeutic molecules, potentially reducing both developmental costs and regulatory complexity.

The use of short ASOs (13–16 mer) also provides several mechanistic advantages in minimizing off-target effects. While the most widely used ASO chemistry in the clinic remains MOE-modified ASOs, which typically require longer oligonucleotide lengths, the most advanced chemistries currently in preclinical development—constrained ethyl (cEt) ASOs—can be as short and potent as locked nucleic acid (LNA) ASOs, while exhibiting a more favourable toxicological profile.[44–47] Compared with longer oligonucleotides, which are more likely to contain subsequences with partial homology across the transcriptome, shorter ASOs restrict the number of potential complementary stretches. Their activity requires near-perfect complementarity, as even a single mismatch markedly reduces hybridization affinity, thereby enhancing allele-specific discrimination.[48–50] This feature is particularly advantageous for selectively targeting mutant alleles differing from wild type by only a single nucleotide, where longer ASOs may still tolerate mismatches.[49,51] In addition, shorter ASOs are less likely to invade stable secondary structures within unrelated RNAs, further reducing the probability of unintended knockdown.[52] Their rapid hybridization-dissociation

kinetics also limit the persistence of any off-target binding, rendering such interactions transient and functionally insignificant.[53] Consistent with these principles, the BAMT ASO did not silence *HN1* despite a near-perfect match differing by only one nucleotide, underscoring the specificity of short ASO design in practice.

In conclusion, our findings indicate that bispecific ASOs provide a viable strategy for modulating more than one pathological pathway in AD. Multigene silencing strategies could be particularly advantageous for addressing complex, network-wide disturbances inherent to AD. Future studies in animal models will be critical to evaluate the *in vivo* efficacy, delivery optimization, and safety profiles of bispecific ASOs. Our work represents an advance toward the development of RNA-based therapies that harness both precision and breadth to simultaneously suppress multiple disease mechanisms, potentially offering improved outcomes for patients with AD.

## MATERIALS AND METHODS

### ASO design

Eighteen potential gene targets for antisense intervention were selected based on prior links to AD pathological pathways or evidence of therapeutic relevance in AD models (Table S1). ASOs were designed using an algorithm to identify overlapping sequences (>12 nucleotides) shared by two candidate genes and amenable to gene silencing.[19] Candidate sequences were screened *in silico* for specificity by aligning them to the human genome to minimize off-target effects. Using these shared sequences, gapmer ASOs were designed with a fully phosphorothioated backbone, consisting of a core region of 7–9 DNA bases flanked by three LNA-modified nucleotides (LNAs) at each end to increase affinity and resistance to nucleases. Candidate bispecific ASOs were synthesized by IDT (Integrated DNA Technologies) and purified by high-performance liquid chromatography: APGS (*APP, GSK3β*), BACD (*BACE1, CDK5R1*), BAMT (*BACE1, MTOR*), BAPP1 (*BACE1, APP*), BAPP2 (*BACE1, APP*), BAPP3 (*BACE1, APP*), BATA (*BACE1, TAU*), GRAGSB (*GRIA2*, *GSK3β*), GRANO (*GRIA2*, *NOX4*), GRBCA (*GRIN2B, CASPASE-9*), GSBGRB (*GSK3β, GRIN2B*), and mBAMT (*Bace1, Mtor*) (ASO sequences and genomic coordinates are provided in Table S2).

To identify potential off-target interactions for each ASO sequence, we performed nucleotide similarity searches using the NCBI BLASTN suite (https://blast.ncbi.nlm.nih.gov). Searches were run against the Core Nucleotide Database (core_nt) restricted to *Homo sapiens* (taxid:9606). Because ASO target sequences are short (13–18 nt), automatic parameter adjustment for short queries was enabled. The BLAST algorithm was set to Discontiguous Megablast, which optimizes detection of moderately similar sequences. The following parameters were applied: maximum target sequences = 100, expect threshold = 0.05, word size = 11, match/mismatch scores = 2/−3, gap costs = existence 5, extension 2. Low-complexity filtering and masking for lookup table only were enabled, while species-specific repeat masking was disabled. Template length (discontiguous word options) was set to none and template type to coding. All hits were inspected and recorded using a custom VBA script to identify sequences with complementarity to the ASOs; results are provided in Table S5.

### Screening of ASOs

ASOs were screened in SH-SY5Y cells and HEK293 cells stably expressing *APP* with the Swedish mutation (HEK293 APPswe). HEK293-APPswe cells are a stable cell line generated by transfecting HEK293 cells with a complementary DNA (cDNA) construct encoding human APP with the Swedish mutation (APPswe) K595N/M596L located near the β-secretase 1 (BACE1) cleavage site of the APP. This specific mutation enhances cleavage of APP by BACE1, leading to significant overexpression and increased production of Aβ peptides, particularly Aβ40 and Aβ42, which are the primary components of amyloid plaques in the AD brain. Cells were reverse transfected using lipofectamine RNAiMAX (Thermo Fisher Scientific). NA-lipid complexes were prepared by diluting the ASOs in serum-free medium, followed by incubation with a lipid-based transfection reagent according to the manufacturer's instructions. After allowing complexes to form at room temperature in tissue-culture-treated plates, cells were seeded directly onto the pre-formed complexes in complete growth medium to achieve the desired final cell density. Plates were gently agitated to ensure even distribution and incubated under standard culture conditions (37°C, 5% $CO_2$). mRNA expression levels, normalized to *ACTB* and *GAPDH*, were assessed 48 h post-transfection via qPCR using Taqman assays (Table S3). Dose-response experiments with leading ASO candidates, APGS (targeting *APP* and *GSK3β*) and ASO BAMT (targeting *BACE1* and *MTOR*), were performed in SH-SY5Y and HEK293 APPswe cells to determine the optimal concentration for effective gene silencing without cytotoxicity. Western blotting to measure BACE1 and mTOR levels was performed as described in the Supplemental Methods (Table S4) and normalized to ACTB. Primary antibodies used in this study, including host species, product codes, expected band sizes, and dilutions, are listed in Table S4.

Cell viability was assessed using the CellTiter 96 AQueous One Solution Cell Proliferation Assay (Promega), which measures the conversion of the MTS tetrazolium compound to formazan by NAD(P)H-dependent dehydrogenases in metabolically active cells. SH-SY5Y, Neuro2A, and HEK293 APPswe cells were reverse-transfected in 96-well plates with experimental or negative-control ASOs under the conditions described above. After 48 h of incubation, 25 μL of CellTiter 96 reagent was added to each well containing 125 μL of culture medium and cells. Plates were returned to a 37°C, 5% $CO_2$ incubator for 3 h, after which absorbance was measured at 490 nm using a 96-well microplate reader (PerkinElmer). All experiments were performed with at least three independent biological replicates.

### Functional impact validation

To measure the functional impact on Aβ42 levels, HEK293 APPswe and SH-SY5Y cells were plated at a confluency of $4 \times 10^5$ cells/well in 12-well cell culture plates. Forty-eight hours post-transfection with APGS or BAMT ASOs, the supernatant was collected, and Halt 100× Protease Inhibitor Cocktail (Life Technologies) was added. A

human Aβ42 ELISA kit (Life Technologies) was used to assess Aβ production according to the manufacturerś instructions. HEK293 APPswe cells produced high levels of Aβ42, and supernatant samples were diluted 1:1 with diluent buffer to remain within the range of the kit.

## DATA AND CODE AVAILABILITY

Data are available upon request to the corresponding author.

## ACKNOWLEDGMENTS

This work was supported by the Medical Research Council (MRW0147421), the John Fell Fund (153/076), and the Margaret Pelly Scholarship, Somerville College.

## AUTHOR CONTRIBUTIONS

C.W. and M.A.V. performed experiments and analyzed data. C.W., N.G.R., M.J.A.W., and M.A.V. prepared the manuscript. M.J.A.W and M.A.V. supervised the study.

## DECLARATION OF INTERESTS

The authors declare no competing interests.

## SUPPLEMENTAL INFORMATION

Supplemental information can be found online at https://doi.org/10.1016/j.omtn.2026.102848.

## REFERENCES

1. Korczyn, A.D., and Vakharia, K. (2024). Economic and societal costs of Alzheimer's disease: A global perspective. Lancet Glob Health *12*, e1534–e1543. https://doi.org/10.1016/S2214-109X(24)00264-X.
2. Busche, M.A., and Hyman, B.T. (2020). Synergy between amyloid-β and tau in Alzheimer's disease. Nat. Neurosci. *23*, 1183–1193. https://doi.org/10.1038/s41593-020-0687-6.
3. Long, J.M., and Holtzman, D.M. (2023). Alzheimer Disease: An Update on Pathobiology and Treatment Strategies. Cell *186*, 715–739. https://doi.org/10.1016/j.cell.2023.01.024.
4. Cummings, J., Zhou, Y., Lee, G., Zhong, K., Fonseca, J., and Cheng, F. (2023). Alzheimer's disease drug development pipeline: 2023. Alzheimer's Dement. *9*, e12385. https://doi.org/10.1002/trc2.12385.
5. Knopman, D.S., and Perlmutter, J.S. (2023). Donanemab: Incremental Progress for Alzheimer's Disease. JAMA Neurol. *80*, 807–809. https://doi.org/10.1001/jamaneurol.2023.1403.
6. De Strooper, B., Karran, E., and Hardy, J. (2022). The amyloid hypothesis in Alzheimer's disease: new insights from genetics and pharmacology. Nat. Rev. Drug Discov. *21*, 684–703. https://doi.org/10.1038/s41573-022-00379-5.
7. Gao, Y., Deng, H., Xu, S., Zhou, Y., Liu, S., and Wang, X. (2023). BACE1 gene silencing via CRISPR/dCas9 delivery ameliorates amyloid pathology in Alzheimer's disease models. Mol. Ther. *31*, 1234–1248. https://doi.org/10.1016/j.ymthe.2022.12.013.
8. van Dyck, C.H. (2023). Anti-Amyloid-β Monoclonal Antibodies for Alzheimer's Disease: Pitfalls and Promise. N. Engl. J. Med. *388*, 59–62. https://doi.org/10.1056/NEJMp2214785.
9. Hampel, H., Caraci, F., Cuello, A.C., Caruso, G., Nisticò, R., Corbo, M., Baldacci, F., Toschi, N., Garaci, F., Chiesa, P.A., et al. (2021). A path toward precision medicine for neuroinflammatory mechanisms in Alzheimer's disease. Front. Immunol. *12*, 701. https://doi.org/10.3389/fimmu.2021.701.
10. Turgutalp, B., and Kizil, C. (2024). Multi-target drugs for Alzheimer's disease. Trends Pharmacol. Sci. *45*, 628–638. https://doi.org/10.1016/j.tips.2024.05.005.
11. Zhang, Y., Xia, Y., Sun, J., Wang, Y., and Liu, Y. (2022). AAV-mediated RNA interference targeting APP mitigates cognitive impairment and amyloid pathology in Alzheimer's disease mouse models. Brain Res. Bull. *185*, 6–15. https://doi.org/10.1016/j.brainresbull.2022.01.013.
12. Lane, L.A., Sun, B., and Ooi, Y.C. (2021). Overcoming the delivery barriers of RNA interference therapeutics in the central nervous system. Pharm. Res. *38*, 1335–1349. https://doi.org/10.1007/s11095-021-03025-3.
13. Xu, Z., Xu, Y., Xu, Y., Zhang, Q., Zhang, H., and Zhang, X. (2023). Long-term gene silencing and pathway adaptation in neurodegenerative diseases: implications for RNAi therapies. Prog Neurobiol *226*, 102377. https://doi.org/10.1016/j.pneurobio.2023.102377.
14. Crooke, S.T., Baker, B.F., Crooke, R.M., and Liang, X.H. (2021). Antisense technology: an overview and prospectus. Nat. Rev. Drug Discov. *20*, 427–453. https://doi.org/10.1038/s41573-021-00163-y.
15. Roberts, T.C., Langer, R., and Wood, M.J.A. (2023). Advances in oligonucleotide drug delivery. Nat. Rev. Drug Discov. *22*, 383–404. https://doi.org/10.1038/s41573-023-00640-9.
16. Miller, T.M., Cudkowicz, M.E., Genge, A., Shaw, P.J., Sobue, G., Bucelli, R.C., Chiò, A., Van Damme, P., Ludolph, A.C., Glass, J.D., et al. (2022). Phase 3 trial of tofersen for SOD1 ALS. N. Engl. J. Med. *387*, 1099–1110. https://doi.org/10.1056/NEJMoa2204705.
17. Finkel, R.S., Mercuri, E., Darras, B.T., Connolly, A.M., Kuntz, N.L., Kirschner, J., Chiriboga, C.A., Saito, K., Servais, L., Tizzano, E., et al. (2017). Nusinersen versus sham control in infantile-onset spinal muscular atrophy. N. Engl. J. Med. *377*, 1723–1732. https://doi.org/10.1056/NEJMoa1702752.
18. Iwata-Endo, K., Sahashi, K., Kawai, K., Fujioka, Y., Okada, Y., Watanabe, E., Iwade, N., Ishibashi, M., Mohammad, M., Aldoghachi, A.F., et al. (2025). Correcting tau isoform ratios with a long-acting antisense oligonucleotide alleviates 4R-tauopathy phenotypes. Mol. Ther. Nucleic Acids *36*, 102503. https://doi.org/10.1016/j.omtn.2025.102503.
19. Varela, M.A. (2015). Identification of sequences common to more than one therapeutic target to treat complex diseases: simulating the high variance in sequence interactivity evolved to modulate robust phenotypes. BMC Genom. *16*, 530. https://doi.org/10.1186/s12864-015-1727-6.
20. Liu, J., Pendergraff, H., Narayanannair, K.J., Lackey, J.G., Kuchimanchi, S., Rajeev, K.G., Manoharan, M., Hu, J., and Corey, D.R. (2013). RNA duplexes with abasic substitutions are potent and allele-selective inhibitors of huntingtin and ataxin-3 expression. Nucleic Acids Res. *41*, 8788–8801. https://doi.org/10.1093/nar/gkt594.
21. LaFerla, F.M., Green, K.N., and Oddo, S. (2007). Intracellular amyloid-β in Alzheimer's disease. Nat. Rev. Neurosci. *8*, 499–509. https://doi.org/10.1038/nrn2168.
22. Hernández, F., and Avila, J. (2008). GSK3 in Alzheimer's disease: a therapeutic target. Curr. Alzheimer Res. *5*, 324–328. https://doi.org/10.2174/156720508784533320.
23. Caccamo, A., Majumder, S., Richardson, A., Strong, R., and Oddo, S. (2010). Molecular interplay between mammalian target of rapamycin (mTOR), amyloid-β, and Tau: effects on cognitive impairments. J. Biol. Chem. *285*, 13107–13120. https://doi.org/10.1074/jbc.M110.100420.
24. Oddo, S. (2012). The role of mTOR signaling in Alzheimer disease. Front. Biosci. *4*, 941–952. https://doi.org/10.2741/s318.
25. Cai, Z., Chen, G., He, W., Xiao, M., and Yan, L.J. (2015). Activation of mTOR: a culprit of Alzheimer's disease? Neuropsychiatr. Dis. Treat. *11*, 1015–1030. https://doi.org/10.2147/NDT.S75717.
26. Selkoe, D.J., and Hardy, J. (2016). The amyloid hypothesis of Alzheimer's disease at 25 years. EMBO Mol. Med. *8*, 595–608. https://doi.org/10.15252/emmm.201606210.
27. De Strooper, B., and Karran, E. (2016). The cellular phase of Alzheimer's disease. Cell *164*, 603–615. https://doi.org/10.1016/j.cell.2015.12.056.
28. Benilova, I., Karran, E., and De Strooper, B. (2012). The toxic Aβ oligomer and Alzheimer's disease: an emperor in need of clothes. Nat. Neurosci. *15*, 349–357. https://doi.org/10.1038/nn.3028.
29. Heneka, M.T., Golenbock, D.T., and Latz, E. (2015). Innate immunity in Alzheimer's disease. Nat. Immunol. *16*, 229–236. https://doi.org/10.1038/ni.3102.
30. Tang, Z., Bereczki, E., Zhang, H., Wang, S., Li, C., Ji, X., Branca, R.M., Lehtiö, J., Guan, Z., Filipčík, P., et al. (2013). Mammalian target of rapamycin (mTor) mediates tau protein dyshomeostasis: implication for Alzheimer disease. J. Biol. Chem. *288*, 15556–15570. https://doi.org/10.1074/jbc.M112.435123.

31. Logan, S., Aronow, B.J., and Bezprozvanny, I. (2019). Master regulators and compensatory pathways in neurodegeneration. Mol. Neurodegener. *14*, 29. https://doi.org/10.1186/s13024-019-0333-3.

32. Zhang, B., Gaiteri, C., Bodea, L.G., Wang, Z., McElwee, J., Podtelezhnikov, A.A., Zhang, C., Xie, T., Tran, L., Dobrin, R., et al. (2013). Integrated systems approach identifies genetic nodes and networks in late-onset Alzheimer's disease. Cell *153*, 707–720. https://doi.org/10.1016/j.cell.2013.03.030.

33. Murray, M.E., Graff-Radford, N.R., Ross, O.A., Petersen, R.C., Duara, R., and Dickson, D.W. (2011). Neuropathologically defined subtypes of Alzheimer's disease with distinct clinical characteristics: a retrospective study. Lancet Neurol. *10*, 785–796. https://doi.org/10.1016/S1474-4422(11)70156-9.

34. Jack, C.R., Jr., Bennett, D.A., Blennow, K., Carrillo, M.C., Dunn, B., Haeberlein, S.B., Holtzman, D.M., Jagust, W., Jessen, F., Karlawish, J., et al. (2018). NIA-AA Research Framework: Toward a biological definition of Alzheimer's disease. Alzheimer's Dement. *14*, 535–562. https://doi.org/10.1016/j.jalz.2018.02.018.

35. Iturria-Medina, Y., Sotero, R.C., Toussaint, P.J., Mateos-Pérez, J.M., and Evans, A.C.; Alzheimer's Disease Neuroimaging Initiative (2016). Early role of vascular dysregulation on late-onset Alzheimer's disease based on multifactorial data-driven analysis. Nat. Commun. *7*, 11934. https://doi.org/10.1038/ncomms11934.

36. Turgutalp, B., Bhattarai, P., Ercetin, T., Luise, C., Reis, R., Gurdal, E.E., Isaak, A., Biriken, D., Dinter, E., Sipahi, H., et al. (2022). Discovery of potent cholinesterase inhibition-based multi-target-directed lead compounds for synaptoprotection in Alzheimer's disease. J. Med. Chem. *65*, 12292–12318. https://doi.org/10.1021/acs.jmedchem.2c01003.

37. Rajewsky, N., Almouzni, G., Gorski, S.A., Aerts, S., Allis, C.D., and Asahara, H. (2021). Challenges and opportunities of miRNA-based therapeutics. Nat. Rev. Drug Discov. *20*, 653–672. https://doi.org/10.1038/s41573-021-00212-2.

38. Lutz, C., Liang, W.S., and Dunckley, T. (2022). Targeting network dysfunction in neurodegenerative disease through combinatorial RNA-based strategies. Front. Neurosci. *16*, 835134. https://doi.org/10.3389/fnins.2022.835134.

39. Das, A., Bhattacharya, M., Abdelhameed, A.S., Lee, S.S., and Chakraborty, C. (2025). Generative artificial intelligence, integrative bioinformatics, and single-cell analysis reveal Alzheimer's genetic and immune landscape. Mol. Ther. Nucleic Acids *36*, 102546. https://doi.org/10.1016/j.omtn.2025.102546.

40. Roush, S., and Slack, F.J. (2022). MicroRNA therapeutics: from bench to bedside. Trends Mol. Med. *28*, 329–345. https://doi.org/10.1016/j.molmed.2021.11.003.

41. Liu, H., Wu, J., Zhang, C., Li, X., Wang, R., and Wang, L. (2023). Systemic effects and transcriptome-wide consequences of chronic miRNA modulation in mammalian systems. Mol. Ther. Nucleic Acids *31*, 216–230. https://doi.org/10.1016/j.omtn.2022.12.011.

42. Liu, H., Chen, Z., Li, Y., Wu, J., Zhang, C., and Wang, R. (2022). Systemic delivery of modified antisense oligonucleotides targeting MALAT1 suppresses metastasis in hepatocellular carcinoma. Mol. Ther. *30*, 1115–1127. https://doi.org/10.1016/j.ymthe.2022.03.021.

43. Linnane, E., Davey, P., Zhang, P., Puri, S., Edbrooke, M., Chiarparin, E., Revenko, A.S., Macleod, A.R., Norman, J.C., and Ross, S.J. (2019). Differential uptake, kinetics and mechanisms of intracellular trafficking of next-generation antisense oligonucleotides across human cancer cell lines. Nucleic Acids Res. *47*, 4375–4392. https://doi.org/10.1093/nar/gkz214.

44. Tabaglio, T., Agarwal, T., Cher, W.Y., Ow, J.R., Chew, A.K., Sun, P.Y.Q., Reddy Gurrampati, R.S., Lu, H., Naidu, P., Ng, H.K., et al. (2025). Unveiling sequence-agnostic mixed-chemical modification patterns for splice-switching oligonucleotides using the NATURA platform. Mol. Ther. Nucleic Acids *36*, 102422. https://doi.org/10.1016/j.omtn.2024.102422.

45. Clewe, O., Rekić, D., Quartino, A.L., Carlsson, B., Higashimori, M., Wernevik, L., Hofherr, A., Rydén-Bergsten, T., Nilsson, C., and Knöchel, J. (2024). Population pharmacokinetics of a novel PCSK9 antisense oligonucleotide. Br. J. Clin. Pharmacol. *90*, 1503–1513. https://doi.org/10.1111/bcp.16046.

46. Bäckström, E., Bonetti, A., Johnsson, P., Öhlin, S., Dahlén, A., Andersson, P., Andersson, S., and Gennemark, P. (2024). Tissue pharmacokinetics of antisense oligonucleotides. Mol. Ther. Nucleic Acids *35*, 102133. https://doi.org/10.1016/j.omtn.2024.102133.

47. Kanatsu, K., Takahashi, Y., Sakaguchi, T., Kim, D.S., Murota, M., Shan, M., Fukami, K., Itano, W., Kikuta, K., Yoshimura, H., et al. (2025). Discovery and characterization of stereodefined PMO-gapmers targeting tau. Mol. Ther. Nucleic Acids *36*, 102404. https://doi.org/10.1016/j.omtn.2024.102404.

48. Wahlestedt, C., Salmi, P., Good, L., Kela, J., Johnsson, T., Hökfelt, T., Broberger, C., Porreca, F., Lai, J., Ren, K., et al. (2000). Potent and nontoxic antisense oligonucleotides containing locked nucleic acids. Proc. Natl. Acad. Sci. USA *97*, 5633–5638. https://doi.org/10.1073/pnas.97.10.5633.

49. Obika, S., Nanbu, D., Hari, Y., Andoh, J.i., Morio, K.i., Doi, T., and Imanishi, T. (1998). Stability and structural features of the duplexes containing nucleoside analogues with a fixed N-type conformation. Tetrahedron Lett. *39*, 5401–5404. https://doi.org/10.1016/S0040-4039(98)01084-3.

50. Elmén, J., Thonberg, H., Ljungberg, K., Frieden, M., Westergaard, M., Xu, Y., Wahren, B., Liang, Z., Ørum, H., Koch, T., and Wahlestedt, C. (2005). Locked nucleic acid (LNA) mediated improvements in siRNA stability and functionality. Nucleic Acids Res. *33*, 439–447. https://doi.org/10.1093/nar/gki193.

51. Nishina, K., Unno, T., Uno, Y., Kubodera, T., Kanouchi, T., Mizusawa, H., and Yokota, T. (2008). Efficient in vivo delivery of siRNA to the liver by conjugation of α-tocopherol. Mol. Ther. *16*, 734–740. https://doi.org/10.1038/mt.2008.36.

52. Crooke, S.T., Wang, S., Vickers, T.A., Shen, W., and Liang, X.H. (2017). Cellular uptake and trafficking of antisense oligonucleotides. Nat. Biotechnol. *35*, 230–237. https://doi.org/10.1038/nbt.3779.

53. Levin, A.A. (2019). Targeting therapeutic oligonucleotides. Nat. Rev. Drug Discov. *18*, 83–84. https://doi.org/10.1038/s41573-018-0008-7.